Molecular Crystals and Liquid Crystals

Publication details, including instructions for authors and subscription information:
http://www.tandfonline.com/loi/gmcl20

Relaxation of Surface Stabilised Antiferroelectric Liquid Crystals at Video Frequency

M. A. Geday [a], P. L. Castillo [a], B. Bellini [a], N. Bennis [a], X. Quintana [a], F. J. López [a] & J. M. Otón [a]

[a] Dpto. Tecnología Fotónica, ETSI Telecomunicación, Universidad Politécnica de Madrid, Ciudad Universitaria s/n, Madrid, Spain

Version of record first published: 31 Aug 2006

To cite this article: M. A. Geday, P. L. Castillo, B. Bellini, N. Bennis, X. Quintana, F. J. López & J. M. Otón (2006): Relaxation of Surface Stabilised Antiferroelectric Liquid Crystals at Video Frequency, Molecular Crystals and Liquid Crystals, 450:1, 1/[201]-15/[215]

To link to this article: http://dx.doi.org/10.1080/15421400600586326

Mol. Cryst. Liq. Cryst., Vol. 450, pp. 1/[201]–15/[215], 2006

ISSN: 1542-1406 print/1563-5287 online
DOI: 10.1080/15421400600586326

Taylor & Francis
Taylor & Francis Group

Relaxation of Surface Stabilised Antiferroelectric Liquid Crystals at Video Frequency

M. A. Geday
P. L. Castillo
B. Bellini
N. Bennis
X. Quintana
F. J. López
J. M. Otón
Dpto. Tecnología Fotónica, ETSI Telecomunicación, Universidad Politécnica de Madrid, Ciudad Universitaria s/n, Madrid, Spain

As part of our line of research into high resolution, video rate antiferroelectric displays we have studied the ferroelectric – antiferroelectric relaxation that follows the data pulse, in surface stabilised antiferroelectric liquid crystal (AFLC) displays, driven by biasless or low bias video frequency waveforms. This generally incomplete relaxation reduces the intensity of the light transmitted by a pixel in any partially ferroelectric (grey-level) state during a video frame, and hence limits the frame-averaged brightness of the AFLC display. The relaxation is a function of the surface stabilisation (i.e., the anchoring strength, pre-tilt and thickness of the device and the pitch of the AFLC), the rotational viscosity of the AFLC, the degree of relaxation of the AFLC between successive frames, the magnitude of the data pulse (grey level) and bias voltage. We have optimised the driving scheme for a number of symmetric and asymmetric (biasless) displays with different antiferroelectric materials and a variety of alignment surfaces, and present mathematical fits to the decaying transparency during single frames as functions of the data pulse. Finally we discuss the mechanisms governing the relaxation.

Keywords: antiferroelectric liquid crystal; video frequency relaxation model

Address correspondence to M. A. Geday, Dpto. Tecnología Fotónica, ETSI Telecomunicación, Universidad Politécnica de Madrid, Ciudad Universitaria s/n, E-28040 Madrid, Spain. E-mail: morten@tfo.upm.es

INTRODUCTION

Antiferroelectric liquid crystals (AFLC) cells are prepared using aligning materials that direct the orientation of the liquid crystal smectic layers. Typically top and bottom electrodes of the cell are coated with identical alignment material. Such cells show an electro-optical response where the Voltage-Transmission curve is symmetric about 0 V, i.e., the optical response for a positive voltage X is identical to that of a negative voltage –X. The hysteresis lobes, intrinsic to antiferroelectric materials, are symmetrically placed with respect to 0 V.

AFLCs that have been sandwiched between two non-identical aligning surfaces show generally an electro-optical response, where the hysteresis lobes are shifted by a certain voltage [1], *the electro-optical response is no longer symmetrical about 0 V*. The liquid crystal behaves as if it were subjected to a DC field apart from the field externally applied, and thus, the grey levels of one of the hysteresis lobes are partially stabilised even when applying a zero external voltage.

The reason for this offset is a matter of discussion. In nematic liquid crystals a model based on charge asymmetry within the liquid crystal has been proposed [2] and has been applied to a number of nematic liquid crystal cells. However, this model does not seem to be applicable to AFLCs since a charge separation inside the liquid crystal would be of opposite sign of the driving external voltage, and thus cannot stabilise any grey levels. We are still investigating the origin of the voltage offset.

The scope of this article is the description of the major decay of the intensity in asymmetric cells driven by video frequency waveforms.

EXPERIMENTAL

In this study the two ITO-glass substrates were covered with obliquely evaporated non-stoichiometric SiO_x and rubbed Nylon 6 respectively, as described elsewhere [1] (Fig. 1). The cell was assembled using 1.7 μm spheric glass spacers and was filled with CS-4001 AFLC (Chisso Corporation) in isotropic phase under vacuum. The sample was placed between crossed polarisers in a polarising microscope and the light transmission was measured using a photodetector. The light transmission along with the driving waveform, were recorded using a computer-controlled oscilloscope.

Prior to the study hysteresis curves were obtained at room temperature. The cell was carefully aligned between crossed polarisers such that the two saturated ferroelectric states transmitted an equal amount of light (Fig. 2). Applying a 1 Hz triangular waveform to the cell the electro-optical response at was symmetric about -4 V, the

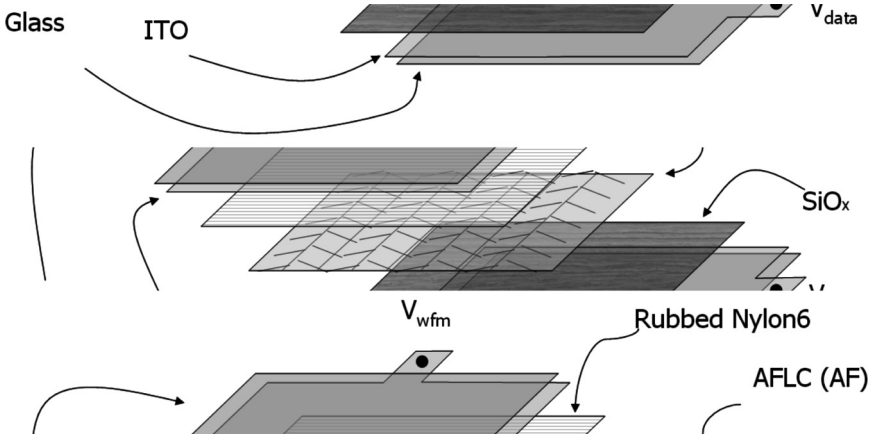

FIGURE 1 Schematic drawing of the asymmetric liquid crystal cell, where one alignment layer is rubbed nylon 6 and the other is SiO_x deposited by oblique evaporation.

response was *shifted* 4 V relative to a symmetric cell. That is, a positive voltage of 10 V applied to the nylon side of the cell would stabilise the grey levels of the positive hysteresis lobe, while a negative voltage of −10 V would be inadequate to stabilise the negative hysteresis lobes. At 0.1 Hz, the shift was 6 V. The displacements are large but within the range seen in similar cells.

During the study the sample was placed inside a hot-stage maintaining a constant temperature of 35°C. The cell was driven by a waveform compatible with a passive multiplexed driving with an elongated bias period. The waveform consisted of a short selection pulse (45 V, 56 μs) followed by a very long biasless period (0 V, 320 ms) and a short DC compensation (−3 V, 840 μs). The driving waveform was applied to one of the electrodes (the nylon side) while a DC-compensated data pulse (0–35 V, 56 μs) was applied to the other (SiO_x). The synchronisation of the two waveforms and the field experienced by the AFLC is shown in Figure 3.

It shall be noted that the described frame is not a video rate driving scheme. The bias period (strictly a biasless period, since no voltage is externally applied) has been intentionally extended well over its actual duration in order to study the long term ($\gg$1 ms) relaxation process for the higher intensities. At video frequency (60 Hz) the total frame duration of the waveform should have been approximately 16.7 ms, not over 320 ms as in the current case. The elongation of bias period was necessary to generate enough data to model the relaxation

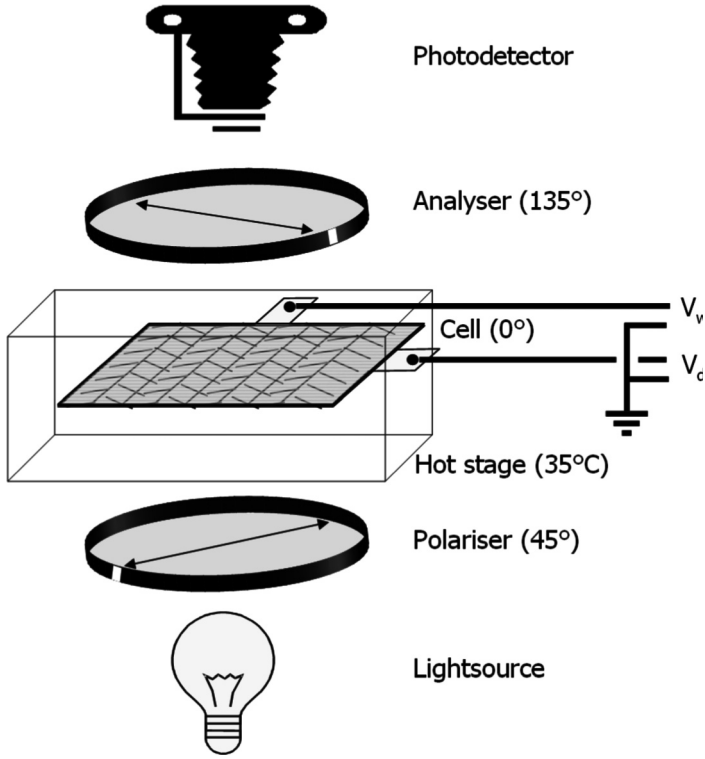

FIGURE 2 The liquid crystal cell placed between the crossed polarisers in the microscope. The smectic layer normal is oriented at 45° with respect to the polariser and analyser. The electrode on the SiO_x face of the cell is wired to the data-line while the the electrode on the Nylon face is wired to the addressing waveform.

which we have found always to be present in bias-less displays driven at 60 Hz. The resulting intensity decay reduces the intensity of the light transmitted by a pixel during a video frame.

The intensity decay from the end of the selection pulse is shown for a number of grey levels in Figure 4, both for the entire bias period and for the initial 16 ms. The field applied during the selection pulse brings the liquid crystal to a bright partial ferroelectric (F) state, (the degree depends on the extent and the magnitude of the pulse). After which the intensity decays during the bias to the dark antiferroelectric (AF) dark state.

A few issues are worth noticing in these decays. The first is that there clearly are two time domains, the initial microsecond during which the cell is undergoing a rapid relaxation, followed by a steadier

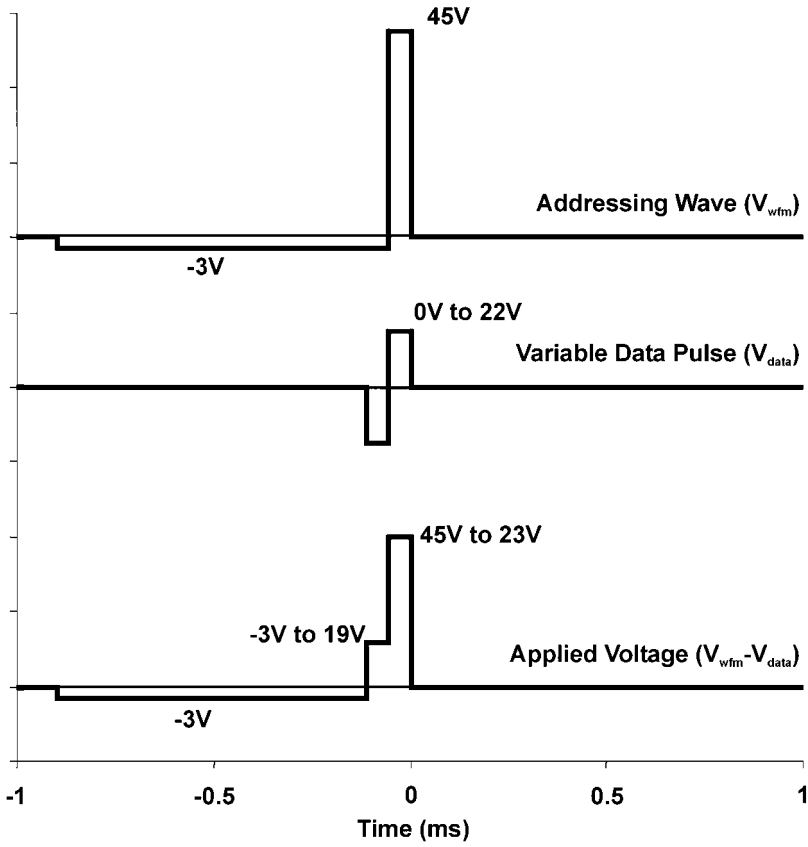

FIGURE 3 a) The DC-compensated driving scheme (waveform) used in the experiments. Only part of the 320 ms long 0 V bias period is shown. b) The DC compensated data line applied to the cell. c) The field experienced by the cell. The magnitude of the applied voltage during selection pulse is often referred to as the selection pulse.

decline in the intensity. The latter relaxation although being slower takes place throughout the normal 16 ms video frame, and thus affects the time averaged frame intensity as much or more than the former. In this study we will concentrate on this, the slower, decay.

The second startling issue is that the intensity decline of the brighter states is significantly slower than that of the darker states. If the measured intensities are translated into ferro- and antiferro-electric populations – i.e., assuming a homogeneous mixture of ferro- and antiferro-electric domains below resolution of the characterisation system – one would expect the system to behave as a decay of an

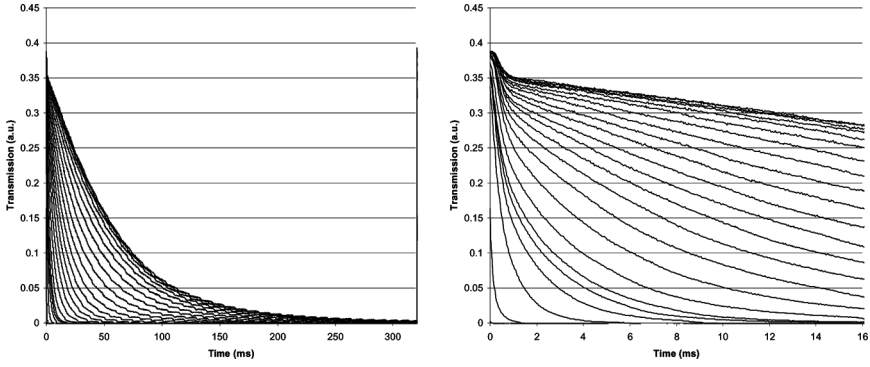

FIGURE 4 Intensity decay for data pulses varying from 0 V to 22 V in steps of 1 V. The uppermost and the lowermost curve correspond to an applied field of 45 V and 23 V respectively. Left: The entire relaxation, Right: The relaxation, as it happens during a 16 ms (60 Hz) video frame.

excited state; i.e., a single exponential decay described by one time constant. Such a simple decay of independent "particles" would have been expected to follow Eq. (1), which is a direct result of combining the Boltzmann distribution with thermal movements of the decaying particles and a certain energy threshold, or activation energy.

$$-\frac{d\Phi(t)}{dt} = K\Phi(t) \tag{1}$$

where Φ(t) is the light transmitting ferro-population, and the decay constant K should be the same for all experiments.

However, the same K was never applicable to datasets representing different grey levels. Thus a simple model of independent particles was not well suited for this problem and a more involved model was required to explain the obtained experimental results.

THE NUMERICAL MODEL

The F→AF relaxation, as seen in the microscope with low frequency signals, develops as a number of thin black lines perpendicular to the rubbing direction that grow parallel to each other while becoming thicker at a much lower rate. It can be derived that ferroelectric domains close to already switched antiferroelectric domains have a much higher chance of fast switching, especially when they share the same smectic layers. AF domains effectively act as "seeds" inducing switching of their neighbours. The idea of calculating the

intensity decay that would occur as a function of initial seedings was in part derived from similar considerations made by [3] working with triangular waveform switching. A numerical model based on these ideas has been created. It consists of the following:

1. A random growth surface (512×512 points), where each point was randomly given a certain *individual switching* "*inertia*" being a value between 0 and 1. A point value of 1 means that the point will switch from F? AF state in the next time slot if one of its neighbours is in an AF state. A value of 0.5 would mean that two slots (or two neighbours) would be needed before switching. For each slot the inertia number is being multiplied by the number of neighbours that is switched, and the point will switch when the sum has reached 1. Each point has 4 neighbours.
2. Random initial seeding. A number of arbitrarily chosen (N) seedings would be done at the beginning of each frame. Some of the seeds will, by chance, be placed at the same point; therefore the number of successful seeds is recorded at the beginning of each simulation. The number of seeds is the only thing varying from simulation to simulation within a series.
3. Anisotropic growth. It is possible to simulate differences in interlayer and intra-layer growth by applying a further inertia factor between growth in one of the directions; i.e., an anisotropy of 0.10 means that a pixel with an individual inertia of 1 would still wait 10 slots before switching if say the vertical neighbour was switched.
4. Spontaneous seeding during the bias time. A number of seeds could occur during the frame. This would happen with a certain probability in each frame.
5. Shuffled, continuous or offset lines. In order to simulate seeds that exits and enters the pixel under observation, various options for shuffling have been investigated in order not to mask slight 2D growth by rapid 1D growth.

A data set is generated by iteration of the frame generation.

Series of dataset showing the decay has been generated, only altering the number of initial seeds. All other parameters were kept constant. During the first simulations it became obvious that it was crucial that the random inertia surface was kept constant during a series of data. Similarly the seeds must be distributed using the same pseudo random series. This is fortunately rather simple to implement since all "random" numbers generated by an algorithm must have an initial number to begin from. Keeping the randomly generated surface and seeding pattern constant reflects also the reality of a static cell.

After thorough investigation of the different parameters of the model it became clear that the simplest 1D model (i.e., no inter smectic layer growth, an anisotropy factor equals 0) where each point has only two neighbours, and where no seeding occurs during the bias, gave the best fit to the experimental data. In this case shuffling or not the successive lines does not affect the result, since there is no 2D growth.

The intensity curves that are the result of the model are all very similar in shape. Stretching the timeslots for one dataset with a large number of initial seeds, it can be made to almost coincide with a dataset with a smaller number of initial seed. This similarity in shape makes it impossible to assign a unique number of seeds to a certain grey level.

Thus there are only two things to fit:

1. The normalisation of the measured data.
2. The timescale relating the seed growth to real time.

In principle a set of time and seed number could be assigned to each measured grey level as can be seen in Figure 5. However, this exact assignment depends on the pseudo random surfaces and seeding patterns used, so it is questionable what information can be derived from such parameters. Notice that the numbers of seeds have been arbitrarily chosen to be a binary series starting at 32. The reason for not including smaller numbers is that the humps like the one visible at the extreme end of the 32 seeds dataset become increasingly dominating with decreasing number of seeds.

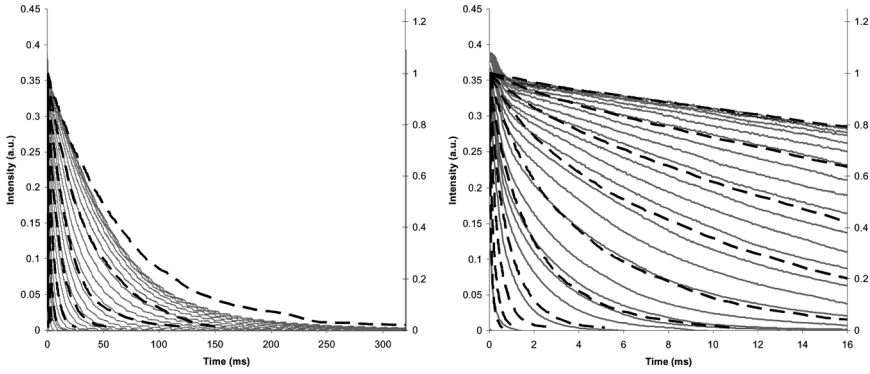

FIGURE 5 Intensity decay as in Figure 4, with the numerical model data overlaid in thick broken lines. The model data has been scaled vertically and horizontally to fit the captured data.

The fit between the model and the data is fair, considering the simplicity of the final model. What supports the model further is the fact that the generated pixel images, not only the measured intensities, appears to correspond to what is seen with low frequency triangular waveform, i.e., needle shaped domain growth [4].

AVRAMI ANALYSIS OF THE DECAY

In order to confirm the one-dimensional growth pattern of the seeds, an Avrami analysis of the decay was performed following the outline of González *et al*. [5]. In crystallisation the Avrami equation [6] describes the fraction of a volume $\varphi(t)$ that is crystallised at a time t. It can be cast as:

$$\ln[1 - \varphi(t)] = -kt^n \tag{2}$$

Assuming that we have only two kinds of domains: dark AF and bright F, and taking $\varphi(t)$ to be the AF fraction we can cast the measured intensity as:

$$\frac{I}{I_0} = 1 - \varphi(t) \tag{3}$$

where I_0 is a hypothetical fully saturated ferroelectric state without any field applied. The value of I_0 can easily be deduced by recasting Eq. (2):

Equation (2) then becomes:

$$\ln\left[\frac{I}{I_0}\right] = \ln[I] - \ln[I_0] = -kt^n \tag{4}$$

Thus the I_0 can be obtained by plotting $\ln[I]$ as a function of t and extrapolating to the value for $t = 0$. This has been done for the entire series of dataset as can be seen in Figure 6. The intersections have been used for the normalisation of each individual dataset.

Upon having determined I_0 it becomes possible to determine n and thereby the character of the domain growth:

$$\ln\left\{-\ln\left[\frac{I}{I_0}\right]\right\} = \ln k + n \ln t \tag{5}$$

As can be seen in Figure 7.

The values for I_0, k and n are summarised in Table 1.

DISCUSSION

We have presented a simple numeric model that to a fair extent mimics the intensity decay of a partially switched antiferroelectric

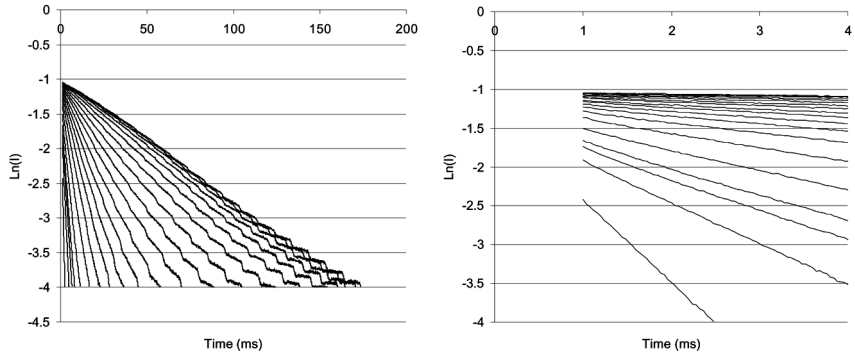

FIGURE 6 ln(I)/Time plot for most of bias period and a reasonably linear part of the curves close to zero, chosen for the estimate of I_0. The lowest values of the intensity ($\ln(I) < -4$) have been omitted due to the noise of the measurements. The first millisecond of the datasets has been omitted as well, since this is deemed to be part of the fast transition. For this reason the datasets corresponding to the two lowest light intensities (23 V and 24 V selection voltage) are not included. The darkest dataset (25 V) correspond to the most inclined curve. The values of the deduced I_0 and the slope of the curves are listed in Table 1.

pixel. The model was found to be working best when using one-dimensional seed growth only. This result is confirmed by the Avrami analysis. This analysis resulted in an exponent of 1 which corresponds to a situation where no additional seeds are generated in time, and the original seeds are growing in one dimension only.

The one-dimensional growth of domains has been illustrated by other authors using stroboscopic light sources to illuminate the sample e.g., Beccherelli and Elston [4].

The direct implication of the numerical model is that the number of seeds depends on the applied voltage. This means that within the pixels, there are various degrees of AF-stabilisation, or various degrees of AF-F phase transition inhibition, such that, upon applying a certain voltage a certain number of AF seeds will still be present. Clearly impurities, such as the spacers used inside the cells, may be a source of such variations, or these variations may in part be the consequence of manufacturing tolerances as previously suggested [7].

In the one dimensional case

$$k = A\rho_n G \tag{6}$$

where A is the average area of the domain cross-section, ρ_n is the nucleation density and G is the speed of growth of the domain. Plotting

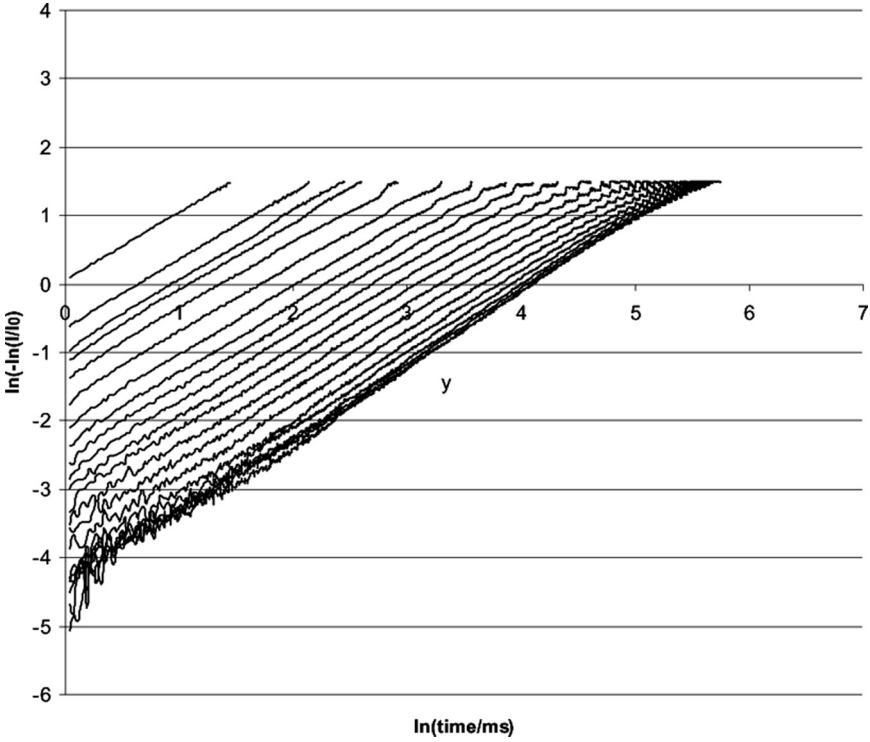

FIGURE 7 $\ln(-\ln(I/I_0))/\ln(\text{Time/ms})$. For the for most of bias period. Values for which $\ln(-\ln(I/I_0)) > 1.5$ all omitted in the fitting of the curves since these low intensity measurements were very much affected by noise. Data corresponding to the first ms has been omitted here. The darkest dataset (25 V) correspond to the top left curve.

$\ln(k)$ against the applied voltage one gets an approximately straight line (Fig. 8); Pearsons R^2-value is larger than 0.99, when making a linear regression to the voltage interval [26 V 41 V], i.e.:

$$\ln k = \beta_0 - \beta_1 V \tag{7}$$

where β_0 and β_1 are the parameters from the linear fit above. Assuming that the growth speed of the AF domains during the bias remains unaltered when applying various fields we can get an expression of the growth surface density ($\Omega(\text{V}) = A\rho_n$) as a function of applied field:

$$\Omega(V) \propto \exp(-\beta_1 V) \tag{8}$$

TABLE 1 Values for the Normalisation of the Datasets (I_0), the Decay Constant and the Decay Exponential as Derived from the Data Shown in Figures 6 and 7

	23 V	24 V	25 V	26 V	27 V	28 V	29 V	30 V	31 V	32 V	33 V	34 V	35 V	36 V	37 V	38 V	39 V	40 V
I_0	0.36	0.26	0.26	0.25	0.25	0.26	0.28	0.30	0.31	0.32	0.33	0.33	0.33	0.34	0.34	0.35	0.35	0.38
k	–	–	1.06	0.53	0.39	0.34	0.26	0.18	0.13	0.1	0.08	0.06	0.05	0.04	0.03	0.03	0.02	0.02
n	–	1.11	0.98	0.98	1.01	1.00	0.95	0.95	0.97	0.98	0.98	0.97	0.95	0.93	0.93	0.94	0.96	0.99

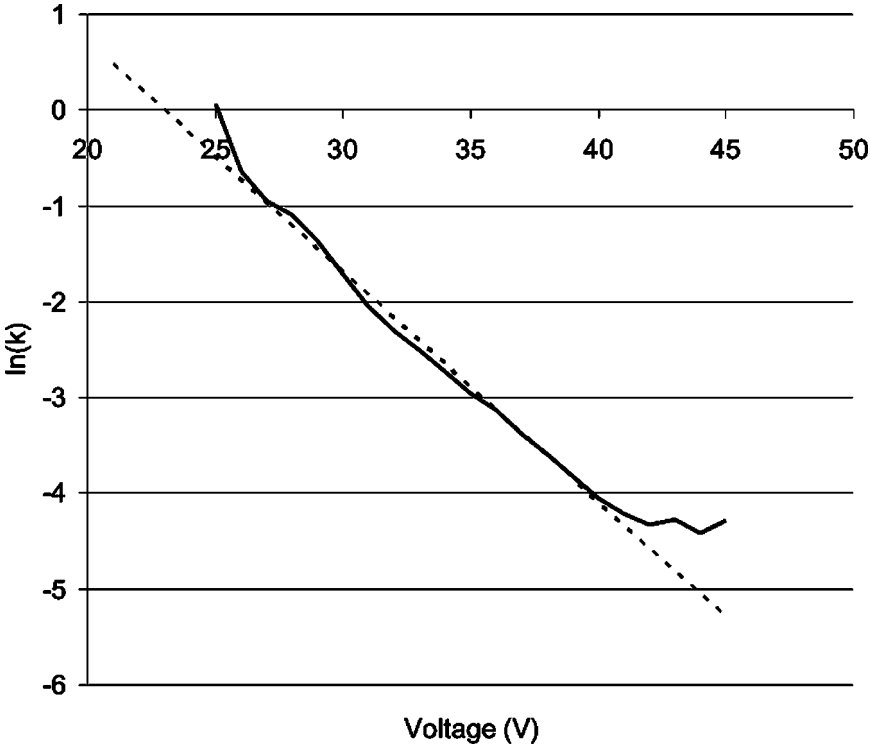

FIGURE 8 Logarithm to decay constant, ln(k), as a function of applied voltage during selection. A linear regression curve made on the interval [26;41] is included. For this interval the R^2-value is better than 0.99.

extending this assumption to the limit, and possibly beyond, of the seed size being independent of the applied field, one can gets a simple expression for ρ_n:

$$\rho_n(V) \propto \exp(-\beta_1 V) \tag{9}$$

It is interesting that domains growth dynamic can be applied, not only to AFLC relaxation, but also to ferroelectric liquid crystals (FLC) switching e.g., [8,9]. In FLC switching the domain growth is driven by a voltage, rather than being a relaxation process. It was found that a 2D-growth model in which both the speed of growth (the domain wall velocity in a two dimension growth model) and the seed density depended on the driving voltage described the behaviour of the FLC well.

In some FLCs ρ_n (the newly created FLC nucleation sites) could be taken to be linearly dependent on the applied field [9]. In our study the nucleation sites are remaining un-switched AFLC domains and thus the seeding origin is very different, and our relationship between voltage and number of seeds is more complex.

Since we do not apply, and hence do not vary, the voltage during the domain growth, we should not expect the voltage dependency of the growth as seen in FLC relaxation.

The Avrami model has also been applied to domain growth during the cooling of a liquid crystal mixture going through FLC-AFLC-crystalline phases [10]. It was found that while a 2D growth model was suitable for the AFLC-crystalline phase transition, then it was unsuitable for the FLC-AFLC phase transition, possibly due to phase separation of the mixture components.

In this paper we have ignored the change in intensity happening during the first ms after the end of selection pulse. The nature of this fast decay is completely different to that of the slow FLC-AFLC phase transition that we have been describing here, and cannot be modelled using the same kind of approach. We believe that the fast decay is related to bulk relaxation of a stressed partial FLC state to a more relaxed partial FLC state, while the FLC-AFLC relaxation described in this is a proper phase transition, where the entire cell content switches, both surface near and bulk molecules. The exact nature of the rapid FLC-FLC relaxation is still under study.

CONCLUSIONS

We have demonstrated that the spontaneous FLC-AFLC relaxation in an AFLC display driven can be modelled using a model in which residual AFLC-seeds are allowed to grow in one dimension only, without any seed generation during the bias period. The result of the numeric model was confirmed using Avrami analysis, which furthermore lead to a somewhat tentative hypothesis that the number of seeds roughly inverse proportional to exponential to the field applied during the selection pulse.

REFERENCES

[1] Gayo, J. L., Otón, J. M., Quintana, X., Urruchi, V., Toscano, C., & Bennis, N. (2002). *Mol. Cryst. Liq. Cryst.*, *375*, 121–127.
[2] Alexe-Ionescu, A. L., Ionescu, A. T., Scaramuzza, N., Strangi, G., Versace, C., Barbero, G., & Bartolino, R. (2001). *Phys. Rev. E*, *64*, 011708.
[3] Parry-Jones, L. A. & Elston, S. (2004). *Mol. Cryst. Liq. Cryst.*, *410*, 141–152.
[4] Beccherelli, R. & Elston, S. J. (1999). *J. Phys. Appl. Phys.*, *D32*, 2241–2245.

[5] González, V. A., Guerrero, C. A., & Aguilar, J. A. (2002). *Ingenierías*, *V15*, 38–43.
[6] Avrami, M. J. (1939). *J. Phys. Chem.*, *7*, 1103.
[7] Sabater, J. & Otón, J. M. (1996). *Liq. Cryst.*, *21*(2), 175–187.
[8] Said, S. M. & Elston, S. J. (2001). *Liq. Cryst.*, *28*(4), 561–571.
[9] Elston, S. J. & Ulrich, D. C. (1995). *J. Appl. Phys.*, *78*, 4331–4338.
[10] Kuczyński, W., Goc, F., & Dabrowski, R. (2001). *Mol. Cryst. Liq. Cryst.*, *366*, 771–784.